Electroabsorption spectroscopy of amorphous Si/SiC quantum well structures

K. Hattori, M. Tsujishita, H. Okamoto, and Y. Hamakawa
Faculty of Engineering Science, Osaka University, Toyonaka, Osaka 560, Japan

(Received 10 April 1989; accepted for publication 9 June 1989)

The interband optical transition in quantum wells of hydrogenated amorphous silicon and silicon carbide has been studied by using electroabsorption (EA) spectroscopy. The observed EA spectrum exhibits a triangular line shape, identified as being due to a field-induced modification of the subband transition. The identification is confirmed by comparing with the experimental result of thermoabsorption spectroscopy.

Electroabsorption (EA) in quantum well (QW) structures consisting of alternate ultrathin layers of crystalline semiconductors has recently attracted much interest both for physics and applications.[1] An electric field perpendicular to the QW layer directly modifies the confined electronic states and corresponding optical transitions. When the potential drop across the layer is small compared to the confinement energy, the optical absorption shifts towards lower photon energy while retaining an abrupt onset. The phenomenon is different in character from a broadening of band-edge absorption due to bulk Franz–Keldysh effect. That is called the quantum-confined Franz–Keldysh (QCFK) effect,[2] or quantum-confined Stark (QCS) effect especially for the excitonic transitions.[1,3,4] Similar phenomena could be expected for the amorphous semiconductor QW structures, in which the quantum confinement effects have been identified experimentally in the differential optical absorption spectra[5,6] as well as in the resonant tunneling characteristics.[7]

In this letter, we report on EA spectrocopy of multiple quantum well (MQW) structures of hydrogenated amorphous silicon (*a*-Si:H) and silicon carbide (*a*-SiC:H). The measured EA spectrum shows a triangular line shape clearly distinguishable from a broad bump-like shape of bulk EA spectrum.[8,9] The feature is identified as due to a subband transition in accordance with a simple model of the QCFK effect assuming a nondirect band-to-band transition.[10] The identification of the EA structure is further supported from the comparison with the thermoabsorption (TA) spectrum measured on the identical MQW structure. Built-in electric field in the well layer is estimated from the relation between the EA signal intensity and the applied field. Applicability of a square QW model for the confined states in the presence of internal field is discussed.

The structure of samples employed for EA measurement was glass/transparent conductive oxide (TCO)/*n*-type *a*-Si:H (400 Å)/undoped MQW of *a*-Si:H and *a*-SiC:H/ *n*-type *a*-Si:H (200 Å)/Al. The *a*-Si:H/*a*-SiC:H MQW structures were prepared by rf plasma chemical vapor deposition with the use of a 1:9 SiH_4-H_2 gas mixture for *a*-Si:H and 1:11:108 SiH_4-CH_4-H_2 gas mixture for *a*-SiC:H. The *a*-Si:H and *a*-SiC:H layers were formed in separate chambers with an interruption on the plasma. In one of the MQWs, the layer thicknesses of the *a*-Si:H well (L_W) and *a*-SiC:H barrier (L_B) were chosen to be 20 and 100 Å, respectively, and the accumulation number of well layers (M) was 150. As a reference structure having different total thickness, a MQW was prepared with $L_W = 20$ Å, $L_B = 60$ Å, and $M = 40$. The multiple layered structures were confirmed to be formed with atomically abrupt heterointerfaces from an x-ray diffraction measurement.[11] The optical band gaps (E_0) were 1.75 eV for *a*-Si:H and 2.8 eV for *a*-SiC:H, respectively. The band discontinuities were estimated to be 0.8 eV for the conduction band and 0.25 eV for the valence band from the results of ultraviolet photoelectron emission measurement.

The electric field modulation was made by the combination of a constant (V_{dc}) and a sinusoidal (V_{ac}) component of voltage applied between Al and TCO electrodes. Positive and negative polarities of voltage refer to the top Al electrode being positively and negatively biased with respect to the bottom TCO electrode. The modulation frequency was fixed at 1 kHz. Here, the effect of current through the MQW is negligible because of the large resistivity perpendicular to the layers, being more than 10^{12} Ω cm. The broadband light with an intensity 1 mW/cm^2 was directed onto the transparent substrate, and the reflected light was dispersed by a monochromator. The reflection R and its modulated component ΔR were detected by a photomultiplier and a lock-in amplifier. The change in transmission of the probe light through the MQW after two passes involving a reflection at the Al electrode makes a dominant contribution to the observed ΔR, as indicated by Nonomura *et al.*[12] The signal defined as a form $-\Delta R/R$ is, therefore, proportional to the field-induced change in absorption coefficient, so far as the spectral region in the vicinity of the absorption edge is concerned.

We will discuss here the EA spectrum expected in the spectral region around the absorption edge, in which the transition between the ground subbands dominates the spectral behavior. It would be reasonable to start with Tauc's model for optical absorption,[11] because it leads to quantitative predictions as simple formulae. The absorption coefficient α in the photon energy region below the onset of the second subband transition is approximately represented by

$$\hbar\omega\alpha = A_1(\hbar\omega - E_1)U(\hbar\omega - E_1), \tag{1}$$

within the context of the model assuming a relaxed selection rule for wave vector k in the direction parallel to the QW layer as well as a constant momentum matrix element for the transition.[5] Here, $\hbar\omega$ denotes photon energy, E_1 is the energy

 0003-6951/89/340763-03$01.00

separation between ground bound states in the conduction band and valence band, and $U(E)$ is a step function. A_1 is a constant proportional to the squared overlap integral of an electron and a hole wave function for the confined states.

The external electric field produces variations in the quantities E_1 and A_1 as follows. In the small field limit, a second-order perturbation approach can be successfully applied,[4] yielding

$$E_1(\Delta F) \cong E_1(0) - \left| \frac{\partial^2 E_1/\partial F^2}{2} \right| \Delta F^2, \tag{2}$$

where ΔF denotes the field perpendicular to the QW layer. Since the electrostatic potential across the QW layer has an odd parity in the confinement direction, a first-order correction term in the perturbation expansion vanishes and does not appear in Eq. (2). The relation shows that the onset energy of the ground subband transition experiences a red shift of an extent proportional to ΔF^2. The quantity A_1 representing the squared overlap integral also follows:

$$A_1(\Delta F) \cong A_1(0) - \left| \frac{\partial^2 A_1/\partial F^2}{2} \right| \Delta F^2. \tag{3}$$

The decrease of A_1 is understood as a natural consequence of the spatial separation of wave functions for electron and hole. The expressions (2) and (3) stand for a low-field limit of the QCFK effect. Field-induced change in absorption spectrum $\Delta\alpha$ is expressed by using Eqs. (1)–(3) as

$$\hbar\omega\Delta\alpha = \left(A_1 \left| \frac{\partial^2 E_1/\partial F^2}{2} \right| - \left| \frac{\partial^2 A_1/\partial F^2}{2} \right| (\hbar\omega - E_1) \right) \times U(\hbar\omega - E_1)\Delta F^2. \tag{4}$$

The important implications of Eq. (4) are that the EA spectrum of the QW has a triangular shape, sharply rising at $\hbar\omega = E_1$ and then decreasing with photon energy, while the magnitude of the signal is proportional to a square of the field strength. In arriving at Eq. (4), we neglect the effect of forbidden subband transitions enhanced due to a broken symmetry under the field. It will produce additional EA structures at each forbidden transition energy. Their contributions are, however, considered to be less pronounced compared with that associated with the first allowed transition which produces the triangular line shape.

Figure 1 presents the EA spectrum of the MQW structure ($L_W = 20$ Å, $L_B = 100$ Å, and $M = 150$). For comparison, the TA spectrum[5] measured on the identical MQW structure directly formed on a glass substrate is also shown in this figure. These spectral shapes of QW structure are clearly different from those commonly observed on thick film.[5,8,9] As discussed in our previous paper, the step-like TA spectrum is ascribed to the subband transition, and the energy position of the step edge is identified as the onset energy.[5] On the other hand, the EA spectrum exhibits a triangular line shape, which is in agreement with that expected from Eq. (4). The EA signal rapidly decaying towards higher photon energy is partly attributed to the effect of increase in absorption coefficient. The spectral structure is identified as due to the subband transition from a good coincidence of the EA peak and the TA step edge. The vertical bar in the figure indicates the position of the calculated onset energy of the

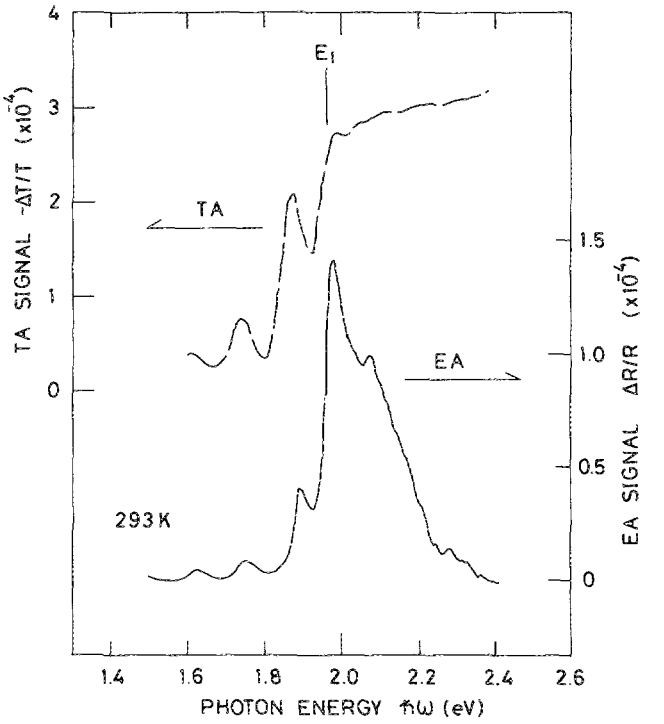

FIG. 1. TA and EA spectra for a-Si:H/a-SiC:H MQW structures with $L_W = 20$ Å, $L_B = 100$ Å, and $M = 150$ at temperature 293 K. The EA spectrum was measured at $V_{dc} = 0$ V and $V_{ac} = 10$ V. The vertical bar indicates the transition energy between the first subbands E_1 calculated from a square QW model.

first subband transition E_1, which agrees well with the energy positions of the TA step-edge and the EA peak. Here, the effective masses for electron and hole were assumed to be 0.3 m_0 and m_0, respectively, in both sublayer regions, where m_0 denotes free-electron mass. These values are identical with those estimated from our recent work on differential absorption spectroscopies of a-Si:H-based QW structures.[5,6]

Roxlo *et al.* have recently studied the EA spectra of a-Si:H($E_0 = 1.77$ eV)/a-SiC:H($E_0 = 2.22$ eV) superlattice structures.[13] The spectral behaviors did not exhibit any features distinguishable from that of bulk materials in contrast to the present result. The disagreement may result from the difference in sample structures used in each experiment. In the combination of well and barrier materials adopted by Roxlo *et al.*, the discontinuity in the valence band is close to zero, so that the QW effect for holes is negligible. In addition, since the widths of the well and barrier layer are set equal to each other, QW levels in the conduction band are broadened with decreasing the sublayer width due to the tunnel coupling. These effects would explain why their EA spectra exhibit no definite features ascribed to QW effects.

Figure 2 shows the EA signal intensity as a function of dc bias voltage V_{dc} for the MQW sample ($L_W = 20$ Å, $L_B = 60$ Å, and $M = 40$). Here, the modulation voltage V_{ac} was held at 2 V. The spectra measured at $V_{dc} = -8$, 0, and 8 V are given in the inset The spectra are found to have an expected triangular shape, when one neglects bumps seen around 1.5 and 2 eV due to interference effect. The presented data for signal intensity are normalized by that at 0 V, and the relative values fall within the indicated error bar over the

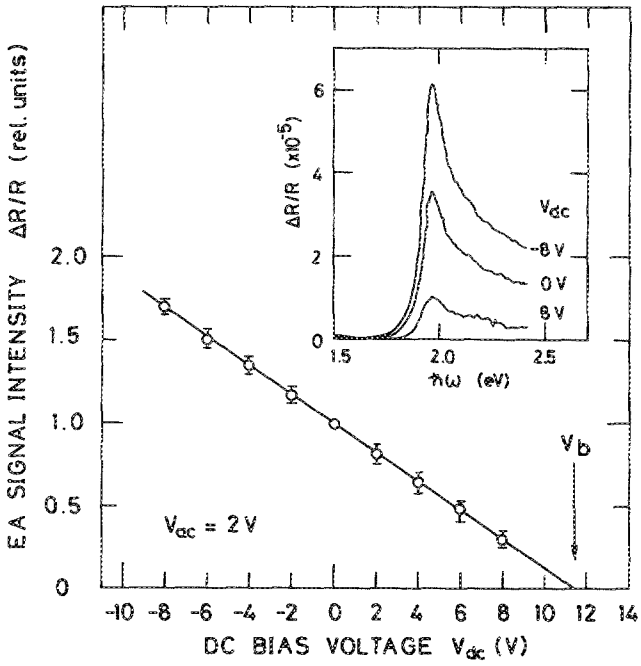

FIG. 2. EA signal intensity measured on a-Si:H/a-SiC:H MQW structure with $L_W = 20$ Å, $L_B = 60$ Å, and $M = 40$ as a function of dc bias voltage V_{dc}. The modulation voltage V_{ac} was held at 2 V. The inset shows the EA spectra for $V_{dc} = -8$, 0, and 8 V.

photon energy region of experiment. Since the EA signal was obtained at the first harmonics of the modulation frequency, the quadratic field-strength dependence leads to a linear relation between the signal intensity and the dc field strength, which is the sum of the applied and built-in fields, so far as the ac field strength is kept constant.[12,14] The excellent linearity found between the EA intensity and the dc bias voltage ensures us that the built-in field is almost independent on the applied dc field. The intercept of the extrapolated line (V_b), thereby, corresponds to the dc bias voltage required to cancel out the built-in potential drop ϕ across each well layer. Simple electrostatics gives the relation between ϕ and V_b: $\phi = V_b[M + (M+1)\epsilon_W L_B/\epsilon_B L_W]^{-1}$, where ϵ_W and ϵ_B are the dielectric constants for well and barrier materials ($\epsilon_W = 12$ and $\epsilon_B = 6.3$). Applying the equation to the experimental data in Fig. 2 yields an estimate of the built-in potential ϕ at 42 mV. The positive ϕ designates a field which points away from the substrate. Assuming that the field is distributed uniformly across the layer, the field strength is measured at 2×10^5 V/cm. An almost identical value was obtained for the sample as in Fig. 1.

Since the estimated built-in field 2×10^5 V/cm is rather large, we have to reexamine the applicability of perturbation theory starting from a square QW model. For this purpose, we have made a numerical calculation of tunneling transmission coefficient through QW structure in the presence of electric field using a transfer matrix technique.[15] The energies of transmission resonance give the positions of the energy levels within the well.[3,4] The results for a QW of 20 Å thickness indicate that the first energy levels for electron and hole both shift downward, with an extent being proportional to the square of electric field F^2 up to around $F = 6\times10^5$ V/cm. Based upon perturbation theory, the quadratic field dependence was applied to the analysis of the EA signal intensity with varying electric field in a range less than 4×10^5 V/cm, as described before. The approach is therefore justified from the numerical result. The calculation also shows that the shift of the transition energy between the first subbands is about 8 meV at $F = 4\times10^5$ V/cm. The shift of such a small extent is likely to be buried in the width of the observed EA spectrum peak, and is considered to be insufficient to be observed in this experimental condition. Therefore, the unperturbed square QW model is a reasonable approximation for the interpretation of the subband transition energy.

The built-in field might be attributed to asymmetrically placed interfacial defects with charge, as suggested by Roxlo *et al.*[14] Following this picture, the interface defect density is estimated to be about 10^{12} cm^{-2} for the present QW system, which is of the similar order as in a-Si:H/a-SiN:H multilayered structures.[14] The extent is larger by one order of magnitude than that of a lattice-matched crystalline superlattice system of GaAs and $Ga_{0.7}Al_{0.3}As$.[16] The presence of defects suggests the increased structural disorder in the interface region, which might work as another source of broadening in energy levels within the QW, in addition to the broadening caused by inherent disorder in the material.

In summary, EA spectrum has been investigated on a-Si:H/a-SiC:H MQW structures. The spectrum exhibits a triangular shape. The behavior is well interpreted as arising from the field-induced modification of the subband transition. The peak energy of EA spectrum gives the transition energy, which is in good agreement with that determined from TA experiment. The built-in potential across the QW layer is estimated to be 42 mV, indicating that the reflection symmetry is slightly broken in the QW potential.

[1] D. A. B. Miller, D. S. Chemla, and S. Schmitt-Rink, in *Optical Nonlinearities and Instabilities in Semiconductors*, edited by H. Haug (Academic, Orlando, 1988), pp. 325–359.
[2] D. A. B. Miller, D. S. Chemla, and S. Schmitt-Rink, Phys. Rev. B **33**, 6976 (1986).
[3] D. A. B. Miller, D. S. Chemla, T. C. Damen, A. C. Gossard, W. Wiegmann, T. H. Wood, and C. A. Burrus, Phys. Rev. B **32**, 1043 (1985).
[4] G. Bastard, in *Interfaces, Quantum Wells, and Superlattices*, edited by C. R. Leavens and R. Taylor (Plenum, New York and London, 1988), pp. 189–209.
[5] K. Hattori, T. Mori, H. Okamoto, and Y. Hamakawa, Phys. Rev. Lett. **60**, 825 (1988).
[6] K. Hattori, T. Mori, H. Okamoto, and Y. Hamakawa, Appl. Phys. Lett. **53**, 2170 (1988).
[7] S. Miyazaki, Y. Ihara, and M. Hirose, Phys. Rev. Lett. **59**, 125 (1987).
[8] Y. Hamakawa, in *Semiconductors and Semimetals*, edited by J. I. Pankove (Academic, New York, 1984), Vol. 21, Part B, pp. 141–158.
[9] G. Weiser, U. Dersch, and P. Thomas, Philos. Mag. B **57**, 721 (1988).
[10] For example, A. Frova and A. Selloni, in *Tetrahedrally-Bonded Amorphous Semiconductors*, edited by D. Adler and H. Fritzsche (Plenum, New York and London, 1985), pp. 271–285.
[11] K. Hattori, T. Mori, H. Okamoto, and Y. Hamakawa, *Advances in Disordered Semiconductors Vol. 1, Amorphous Silicon and Related Materials*, edited by H. Fritzsche (World Scientific, Singapore, 1988), pp. 957–976.
[12] S. Nonomura, H. Okamoto, and Y. Hamakawa, Appl. Phys. A **32**, 31 (1983).
[13] C. B. Roxlo, B. Abeles, and P. D. Persans, Appl. Phys. Lett. **45**, 1132 (1984).
[14] C. B. Roxlo, B. Abeles, and T. Tiedje, Phys. Rev. Lett. **52**, 1994 (1984).
[15] M. O. Vassell, J. Lee, and H. F. Lockwood, J. Appl. Phys. **54**, 5206 (1983).
[16] A. Mauger, S. L. Feng, and J. C. Bourgoin, Appl. Phys. Lett. **51**, 27 (1987).